Title

Nestin in immature embryonic neurons regulates axon growth cone morphology and Sema3a sensitivity

Authors

C.J. Bott[1], C. G. Johnson[2], C.C. Yap[1], N.D. Dwyer[1], K.A. Litwa[2], B. Winckler[1,3].

Address

[1]Department of Cell Biology, University of Virginia, Charlottesville, VA 22908, USA.

[2]Department of Anatomy and Cell Biology, The Brody School of Medicine, East Carolina University, Greenville, NC 27834, USA.

[3] Corresponding Author: bwinckler@virginia.edu

Running title

Unexpected role for nestin in embryonic neurons

Key Words

Intermediate filament, neurofilament, semaphorin, growth cone collapse

Abstract

Nestin is an atypical intermediate filament expressed highly in neural progenitors and is thus used widely as a progenitor marker. Nestin, but not other intermediate filament subtypes, interacts with and regulates cdk5 kinase. Here we surprisingly identify a subpopulation of embryonic cortical neurons which transiently express nestin in their axonal growth cones. Since the repulsive guidance cue Semaphorin 3a (Sema3a) activates cdk5, we tested if nestin-expressing neurons showed altered responses to Sema3a. We find that nestin-expressing neurons are more sensitive to Sema3a, and that nestin knockdown results in lowered sensitivity to Sema3a. We propose that nestin is a modulator of cdk5 in immature neurons leading to an altered Sema3a response. Since correct wiring in the neocortex requires that responses to an individual guidance cue vary among neurons in the same location, and within the same neuron over time, the transient expression of nestin could allow for temporal modulation of a neuron's response to Sema3a, critical for early cortical axon guidance decisions.

Introduction

Proper wiring of the nervous system requires that axonal growth cones respond to a variety of extracellular guidance cues to find their correct targets (Kolodkin & Tessier-Lavigne 2011). Semaphorin 3a (Sema3a) is one of many diffusible developmental cues that has been shown to repel axons of responsive neuronal populations in culture (Sibbe et al. 2007). Addition of Sema3a to cortical neurons causes collapse of many axonal growth cones (Dent 2004). Binding of Sema3a to its receptor neuropilin 1 and co-receptor Plexin A leads to downstream activation of the neuronal Serine/Threonine kinase cyclin dependent kinase 5 (cdk5) (Sasaki et al. 2002). Cdk5 is critical for early neuronal development as a regulator of cytoskeletal, trafficking, and membrane dynamics and thus cell morphology (Kawauchi 2014). Sema3a activated Cdk5 phosphorylates multiple substrates to affect the assembly and dynamics of both the actin and microtubule cytoskeleton and of adhesion components which results in filopodial retraction and growth cone collapse *in vitro* (Sasaki et al. 2002),(Ng et al. 2013). Not all cortical neurons are repelled by Sema3a, and the molecular mechanisms for this differential responsiveness are under active investigation (Carcea et al. 2010; Mintz et al. 2009; Ip et al. 2011). In this work, we find, surprisingly, that the intermediate filament (IF) protein nestin localizes to axonal growth cones of a subpopulation of cortical neurons and imparts increased Sema3a responsiveness to this population.

Intermediate filaments are generally thought to provide structure and stability to a cell, and intermediate filaments in neurons (neurofilaments) provide the structure to maintain axon caliber in adult neurons (Lariviere & Julien 2003). Neurofilaments, alpha-internexin, and vimentin (all expressed in CNS neurons) have also been shown to play additional but poorly understood roles in early neuritogenesis (Shea et al. 1993; Shea & Beermann 1999; Lee & Shea 2014; Walker et al. 2001). Nestin is much larger than conventional intermediate filaments, such as vimentin (57 kD vimentin vs ~280kd nestin), and has a long C-terminal tail, which contains a unique binding and regulatory site for the cdk5 complex (Sahlgren et al. 2003; Sahlgren et al. 2006). In muscle, nestin recruits cdk5 activity to the membrane and regulates agrin-dependent acetylcholine receptor clustering at neuromuscular junctions (Yang et al. 2011). The neuromuscular junction phenotype of the nestin knockout mice phenocopy cdk5 knockout mice (Lin et al. 2005). Similarly, nestin knockdown in cultured C2C12 myotubes abolishes acetylcholine agonist induced cdk5 activity (Yang et al. 2011). These findings suggest that nestin is critical to the function of cdk5 in muscle. Since nestin is one of the most commonly used markers for neural progenitors and not thought to be expressed in neurons, the function of nestin in neurons has not been investigated.

In this work, we first characterized the patterns of endogenous nestin expression and found that it is expressed not only in progenitors, but also in neurons at early developmental time points. Secondly, we found that depletion of nestin with siRNA affects growth cone morphology of immature cortical neurons. Lastly, we discovered

that nestin depletion from cultured neurons decreases their sensitivity to acute, low doses of Sema3a in a cdk5-dependent manner. Based on our data, we propose that nestin acts as a "gain control" modulator of cdk5/Sema3a growth cone signaling during early neuronal differentiation. Since neurons can encounter the same cue at different developmental stages, but respond differently (Kolodkin & Tessier-Lavigne 2011), nestin's modulation of a growth cone's Sema3a responsiveness might be one mechanism to temporally regulate differential axon guidance decisions in the cortex.

Results/Discussion

Nestin protein expression persists in immature primary cortical neurons in culture.

Nestin protein is expressed at high levels in cortical radial glia/neural progenitor cells (NPCs) (Lendahl et al. 1990). In contrast, Doublecortin (DCX) and β3-tubulin expression is low in NPCs but upregulated in postmitotic neurons (Francis et al. 1999). Nestin and DCX/β3-tubulin are thus routinely used as markers to distinguish these mutually exclusive cell types. E16 mouse dissociated cortex was cultured for one day (1DIV = day in vitro) and immunostained against nestin and DCX. To our surprise, many DCX-positive cells were also positive for nestin (Fig.1A). These DCX/nestin-double positive cells had the morphology of stage 3 immature neurons (according to Banker staging (Dotti et al. 1988)) (Fig.1A) and were positive for neuronal-specific β3-tubulin (see below), indicating that they had differentiated into neurons. In stage 2 neurons which do not yet have an elaborated axon, nestin had a non-polarized distribution and was detected in the majority of neurite processes (data not shown). In stage 3 neurons which have specified an axon, nestin was strikingly concentrated at the distal region of the growing axon (pink arrowheads) but was rarely present in secondary neurites (white arrows) (Fig.1A). Low levels of nestin were often also detected in the cell body. In addition to the distal axon accumulation of nestin, short linear nestin profiles were often found distributed along the length of the axon (white arrowhead) (Fig.1A), presumably representing short assembled intermediate filaments (IF) undergoing axonal transport (Wang et al. 2000). The axon-enriched localization of nestin is reminiscent of neurofilaments which are trafficked to the axon by kinesin-1 as short filaments and are rare in dendrites (Xia et al. 1988; Uchida et al. 2009; Holmgren et al. 2013; Yabe et al. 2001).

Because nestin is considered a neural stem cell marker whose expression rapidly disappears from differentiating neurons, we performed a series of rigorous controls to validate the observed staining. We obtained two additional nestin antibodies (raised in Chicken (Chk) or Goat (Gt)), all against different epitopes in the C-terminal region of nestin. Both antibodies produced immunostaining patterns similar to the mouse-anti-nestin antibody (Fig.1A,B). A blocking peptide was available for the goat nestin antibody which allowed testing the specificity of the observed axonal nestin staining. Pre-incubation of the goat anti-nestin antibody with the immunizing peptide

prior to labeling specifically blocked immunostaining with the goat antibody, but nestin was still detected in distal axons with the mouse anti-nestin antibody in the same cell (Fig.1B). As an additional validation of antibody specificity, we performed nestin knockdowns with either control (siCon) or nestin-specific (siNes) siRNAs using Amaxa nucleofection prior to plating dissociated neurons. GFP was co-electroporated to visualize transfected cells (Fig.1C). Cultures were fixed after 36 hrs and stained for nestin. The intensity of axonal nestin was then quantified. At 36 hrs, approximately 1/3 of GFP-positive stage 3 neurons stained positive for nestin after siCon electroporation (similarly to untransfected cells- see below), whereas nestin staining was significantly reduced and essentially undetectable in GFP-positive cells electroporated with siNes (Fig.1C). The specificity of the three nestin antibodies was also assessed by western blot after siRNA knockdown in neurons (Fig.S1A). Since electroporation is not very efficient neurons, the knockdowns were not complete, but decreased nestin levels were found after siNes nucleofection for all three antibodies confirming that they were specific for nestin. When mouse nestin-myc was transfected into HEK293 cells together with either siCon or siNes siRNA, a near complete loss of nestin signal was observed in the siNes treated condition. The IF vimentin was not affected (Fig.S1A), again confirming that the mouse nestin antibody is specific to nestin. We conclude that nestin is indeed expressed in immature neurons in culture. Close reading of the literature uncovered that nestin expression in neurons had in fact been previously reported in a small number of papers, both in early differentiating neurons (Yan et al. 2001; Walker et al. 2007; Crews et al. 2011), as well as in subpopulations of adult human and murine neurons (Hendrickson et al. 2011; Su et al. 2013; Perry et al. 2012). Intriguingly, our experiments show a striking accumulation of nestin in the distal region of developing axons, something that was not previously reported.

To directly compare the nestin levels seen in NPCs (which are known to express high levels of nestin) to those seen in the axons of differentiating neurons, we compared nestin staining between the DCX-positive axon of a neuron and an adjacent NPC (Fig. S1B). Nestin expression of the NPC is many fold brighter than that in the axon. However, when a protrusive process of the NPC containing finer nestin filaments was compared to the intensity of nestin filaments in a DCX-positive axon, the nestin-positive filaments had comparable intensities. Another line scan of the same DCX expressing axon shows a region that lacks any nestin immunoreactivity (Fig. S1B) showing low background immunostaining. We thus reliably detect moderate levels of nestin in DCX- and β3-tubulin positive neurons, albeit several fold lower than in NPCs. High nestin staining is thus still a reliable NPC marker.

Nestin forms mixed intermediate filament (IF) heteropolymers (Steinert et al. 1999) with other IF subunits in other cell types. If axonal nestin was functional in immature neurons, it would be expected to be associated with assembled IFs in the distal axon. Indeed, nestin co-localized with vimentin and neurofilament-M in similar staining patterns (Fig. 1D). A high magnification line-scan of a nestin/neurofilament co-linear filament is shown to better evaluate the extent of co-localization (Fig. 1D). This

pattern is reminiscent of nestin-IF heteropolymers in other cell types where individual subunits occupy distinct subdomains within a heteropolymer (Leduc & Manneville 2017), and suggests that nestin is incorporated into assembled IFs together with other expressed IF subtypes in immature axons.

Nestin-expressing neurons are observed in multiple rodent and human culture models

Since neurons are not usually thought to express nestin, we looked at other neuronal models to see if we observed other instances of DCX/nestin doublepositive neurons. When we prepared neuronal cultures from rat cortex, we also observed DCX/nestin doublepositive neurons (not shown). We then asked whether DCX positive neurons differentiated from NPCs in culture continued to express nestin. We grew mouse NPC's as neurospheres, and then differentiated them into neurons. Differentiation into neurons takes several days using this protocol. One day after neurosphere dissociation and plating, >95% of cells were nestin-positive, but did not express DCX, consistent with them being NPCs (Fig. 2A). The remainder had started to differentiate into neurons and expressed both DCX and nestin. After 4 days of differentiation in dissociated culture, ~50% of cells had differentiated into neurons (DCX-positive). A large proportion of the DCX-positive neurons also expressed nestin. The DCX/nestin doublepositive cells had a morphology similar to stage 2 or stage 3 cultured primary neurons and cells with a stage 3 morphology had nestin localized to the tips of neurites. (Fig. 2A inset). Only around 10% of cells had no detectable nestin immunopositivity (Fig. 2A) and expressed only DCX, consistent with being more differentiated neurons. Differentiating NPCs after 4 days became too crowded to assess on a cell by cell basis.

To test whether human neurons similarly express nestin during early differentiation, we assessed nestin expression in cultures derived from human neural progenitor cells derived from induced pluripotent stem cells (IPSCs). At 1 day, nestin expression is high and βIII tubulin expression is low- resulting in low co-localization of nestin and βIII tubulin. After 4 days of differentiation, nestin colocalization with β3 tubulin peaked, and nestin staining was clearly detected at the tips of β3-tubulin positive axons (Fig. 2B), confirming nestin expression also in cultures of human neurons. Co-localization again drops at ~ 1 week due to decreasing nestin expression, however nestin is still expressed at the tips of some neurites. To assess if nestin expression occurred in neurons that are differentiating in a more tissue-like context, we also grew human NPCs as large cortical spheroids, often referred to as "minibrains" (Fig. S2A). Minibrains recapitulate several developmental processes which are also observed during *in vivo* development. Nestin staining was clearly detected in neurons (identified by β3-tubulin expression). Strikingly, nestin staining was most prominent in neuronal processes with lower β3-tubulin expression (less mature neurons), while cells expressing higher levels of β3-tubulin (more mature neurons) were mostly negative for nestin. Our observations so far are consistent with the model that nestin is transiently

expressed in neurons in both human and rodent neurons, and can be observed in a model that recapitulates cortical human brain development.

Nestin protein is transiently expressed broadly among cortical neuron cell types but decreases with maturation

Typical techniques to culture primary neurons select for cells that just recently completed mitosis, or are undergoing migration at the time of dissociation (Banker & Cowan 1977). We thus wondered if nestin-positive neurons represent a transition state between nestin-positive neural progenitor cells (NPCs) and nestin-negative neurons. Alternatively, nestin-positive neurons could be a stable subset which maintained nestin expression over longer times in culture. Since cultured cortical neurons maintain cell type fates after dissociation (Romito-DiGiacomo et al. 2007; Digilio, L. Yap, CC. Winckler 2015), we used two cell-type specific transcription factors to distinguish cortical (Satb2-positive) from subcortical (CTIP2-positive) neurons. Nestin expression in DCX-positive neurons did not correlate with either CTIP2 or Satb2 expression (Fig. S2B). Similarly, when cultures were prepared from E14, E15 or E16 embryos (representing different cortical layer fates), about 2/3 of DCX-positive neurons were nestin-positive after 24 hours in culture (data not shown), regardless of embryonic age at dissection. These data suggest that nestin is expressed by immature neurons of all cortical layer.

Since nestin-positivity was not skewed by neuronal cell type, we next assessed if nestin expression was correlated with time after differentiation. To this end, we utilized an *in vitro* time course of neurons dissociated from E16 mouse cortex (Fig. 2C). Neurons surviving in primary neuronal cultures are those which had recently undergone cell division (Banker & Cowan 1977), thus time in culture represents the maturity of the cell. For the first 12- 24 hours, around two-thirds of stage 3 neurons express nestin in the axon. When cells were plated at low (half) density (LD), the percentage of stage 3 nestin expressing cells at 24 hrs did not change and is thus not density-dependent. Nestin expression drops steadily after 24 hours, with only one third remaining nestin-positive at 36 hrs and one quarter by 48 hours (Fig. 2C). Average growth cone size and filopodia number increased over this time period, although filopodia number per perimeter remained constant (Fig. S1C). After 72 hours in culture, the cultures became too dense to parse individual neurons, thus we could no longer quantify the percentage of nestin-positive neurons. In order to assess whether nestin-positive axons disappeared completely after more time in culture, we utilized cortical explants that extend axon bundles away from the explant containing the cell bodies. This allows for visualization of an axon bundle for a qualitative assessment of nestin expression. At 36 hours, nestin expression was clearly seen mostly in the distal region of some axons, but was reduced to near background levels at 72 hours (Fig. 2D). These data demonstrate that nestin is expressed transiently in a substantial subpopulation of differentiating cortical axons, and subsequently downregulated as differentiation proceeds.

Nestin is expressed in subpopulations of developing cortical neurons in vivo.

We next sought to determine if there was an *in vivo* correlate to the axonal nestin expression we observed in cultured neurons. We thus imaged axons in the lower intermediate zone (IZ) (Namba et al. 2014) of cryosections of E16 mouse developing cortex, corresponding to recently born neurons that had begun to extend axons. *In vitro*, nestin is not present in all axons and does not fill the whole length of an individual axon. We thus predicted that nestin positive axons would be detected as a subpopulation of axons in the IZ. We also predicted that axonal nestin would be lower than nestin levels in NPCs/radial glia. For orientation, a low magnification overview of one hemisphere of the cortex showing vimentin and α-internexin expression is shown in Fig. 3A, along with a schematic. The boxed region in Fig. 3A indicate the lateral lower IZ which is the region in the schematic imaged in the following panels. All panels in Fig. 3 B-E have the radial glia oriented vertically and axon tracts oriented horizontally. α-internexin is an IF expressed early in neuronal development, but not expressed in radial glia (Kaplan et al. 1990). As expected, α-internexin (INA) is readily detected in axons of the IZ (Fig. 3A,B). Vimentin is expressed in both radial glia and neurons (Boyne et al. 1996; Toth et al. 2008; Yabe et al. 2003).

The high nestin staining intensity in the radial glia (arrowheads in Fig. 3B,C) makes evaluation of nestin staining in axon tracts challenging, however high resolution confocal microscopy, the use of distinct axonal markers, and sequential imaging of four channels permitted us to resolve and distinguish between the segregated but interwoven cellular processes of radial glial and IZ axons. Staining with chicken and goat anti-nestin antibodies labeled the bright radial glia fibers (INA negative) oriented vertically (arrowheads). α-internexin (INA) labels early cortical axon tracts (arrows), and nestin immunoreactivity was clearly detected in these axon tracts, albeit at lower levels compared to radial glia fibers. This staining pattern is similar to what is seen with in vitro axon bundles (Fig. 2D). Early defining work had observed low nestin staining on spinal cord axons, but attributed it to background staining by the antibody (Hockfield & McKay 1985). To assess if the nestin staining on IZ axons is non-specific background, we repeated the peptide blocking assay used in Fig. 1 for the goat anti-nestin antibody on E16 cryosections (Fig. 3B). The staining by the goat nestin antibody was completely blocked by pre-incubation with the immunizing peptide, both on radial glia fibers and on axon tracts, indicating specific staining of nestin on axons in vivo. Both radial glia fibers and axons were still stained with the chicken nestin antibody.

To further characterize the IF content of the lower IZ axons, co-staining for nestin and vimentin was performed (Fig. 3C). Vimentin was found to have a similar staining pattern to nestin, with high levels in radial glia, and low levels in axons. The nestin- and vimentin-positive IZ fibers were also positive for the axon marker L1-CAM (Fig. 3C), confirming their identity as axons. The same axonal nestin staining pattern was seen with the mouse anti-nestin RAT401 monoclonal antibody, the initial antibody to

characterize and define nestin (Hockfield & McKay 1985) (Fig. S2B). We thus provide multiple pieces of evidence (using multiple nestin antibodies and a peptide block assay) to demonstrate that nestin is expressed in axons in the IZ at E16 in mouse cortex.

To better visualize the axonal nestin, we performed STED super-resolution microscopy on goat anti-nestin immunostained tissue. The bright nestin-positive radial glia fibers were again the most prominently stained feature, but individual axons with less bright nestin staining could be unambiguously resolved. Nestin is clearly present on a subset of axons of the IZ (Fig. 3D). At E16, the L1-CAM labels both ascending thalamo-cortical (calretinin-positive) axons and descending cortico-thalamic axons (TAG-1 positive) (Takebayashi et al. 2015) in the IZ. We thus used these three markers to define the nestin expressing sub-population (Fig. 3E). Intriguingly, we observed that a subpopulation of TAG-1 positive (cortical) axons had detectable nestin staining whereas the calretinin-positive (thalamic) axons lacked nestin staining (Fig. 3E).

<u>The level of nestin expression in neurons influences growth cone morphology and response to Semaphorin3a.</u>

An important question is whether nestin plays a functional role in axons, or is simply left over from the mother NPC. Little is known about nestin function generally, even in NPCs (Sahlgren et al. 2006). Nestin function is best understood in muscle development where it acts as a scaffold for cdk5 (Yang et al. 2011; Pallari et al. 2011; Mohseni et al. 2011). Since Sema3a is upstream of cdk5 in neurons (Kobayashi et al. 2014), we wondered if nestin could play a role in modulating growth cone responses downstream of Sema3a. In cultured neurons, growth cone collapse starts within minutes of Sema3a exposure with the loss of growth cone filopodia, resulting ultimately in a collapsed growth cone with no filopodia (Dent 2004).

As a starting point, we determined if axons and growth cones were the same or different in neurons with different levels of nestin expression. We binned neurons into three groups based on nestin intensity in the distal axon, undetectable (-), low (+), and high (++) (representative images in Fig. 4A). Nestin levels were not correlated with any variance in axon length (Fig. 4B), but growth cone area was significantly smaller when nestin was present (Fig. 4C). This morphology was similar to what was seen with tannabin (the nestin homolog in frog) in cultured frog neurons (Hemmati-Brivanlou et al. 1992). When low doses of Sema3a (1nM) were applied for 5 min in the bath, growth cone collapse was observed in about 25% of neurons (Fig. 4E). Sema3a-mediated growth cone collapse was inhibited with pretreatment with the cdk5 inhibitor roscovitine, in agreement with previous work (Sasaki et al. 2002). When neuron populations were binned by nestin expression, growth cone collapse in Sema3a was strikingly correlated with nestin levels (Fig. 4D,F). Neurons not expressing nestin did not collapse within 5 minutes (Fig. 4F).

Prior to complete growth cone collapse, Sema3a leads to retraction of individual filopodia (Dent 2004). In order to quantitatively evaluate this early response to Sema3a and the contribution of nestin in the Sema3a pathway, we counted actin-rich filopodial protrusions of the growth cone (Fig. 4G). In untreated cells, filopodia number was inversely correlated to axonal nestin levels (Fig. 4G), similarly to the smaller growth cone size observed for nestin-positive axons (Fig 4C). After Sema3a treatment, nestin-positive cells retracted growth cone filopodia significantly, whereas nestin-negative growth cones were not significantly affected by Sema3a during the 5 minute timeframe (Fig. 4G). Similarly to total growth cone collapse (Fig. 4E), filopodia retraction in nestin-positive axons was inhibited by the cdk5 inhibitor roscovitine (FigS3B). High magnification insets reveal the nestin filaments consistently appeared fragmented after Sema3a treatment (compare Fig. 4A (high nestin: ++) to Fig. 4D (high nestin:++)). This is in agreement with previous observations in other cell types that cdk5 activation results in nestin phosphorylation and IF disassembly (Sahlgren et al. 2003). Based on these results, we suggest that nestin acts as a modulator downstream of Sema3a signaling.

Nestin depletion results in abnormal growth cone morphology and resistance to Sema3a.

The preceding experiments demonstrate a strong correlation between axonal nestin expression and growth cone size, filopodia number, and Sema3a mediated growth cone collapse. To test for nestin dependence directly, we knocked down nestin with nestin siRNA using Amaxa nucleofection in E16 cortical cultures. GFP was co-transfected to reveal electroporated cells. Control siRNA was used to control for non-specific effects of electroporation of siRNAs. Cells were fixed and assessed after 36 hours in culture (Fig. 5). Nestin siRNA efficiently reduced the number of nestin-positive neurons (see Fig 1B). Axon length, was not statistically different between siCon and siNes treated cells (Fig. 5A,B). As predicted from the inverse relation between endogenous nestin expression and growth cone size (Fig. 4C), cells transfected with siNes had significantly larger growth cones than controls (Fig. 5A,C). After treatment with 1nM Sema3a for 5 minutes (Fig. 5D), ~40% of siCon cells had completely collapsed growth cones, whereas very few growth cones collapsed in the siNes-transfected cells after Sema3a treatment (Fig. 5E). When growth cone filopodia number was quantified in untreated conditions, siNes-transfected cells had significantly higher filopodia on average compared to siCon-transfected cells (Fig. 5F). siCon transfected neurons had a significant reduction in filopodia number following Sema3a treatment, but siNes transfected cells showed no change in filopodia number (Fig. 5F). These results demonstrate surprisingly that nestin greatly increases the sensitivity of axonal growth cones to Sema3a.

Our results have intriguing implications for axon guidance during development, implications that we will pursue in the future. Neural development requires that axonal

growth cones respond to a variety of extracellular guidance cues to change their direction of growth for proper wiring of the nervous system (Kolodkin & Tessier-Lavigne 2011). Importantly, not all growth cones traversing the same environment respond the same way to the same cues (Carcea et al. 2010; Mintz et al. 2009). Even more remarkably, the same growth cone often responds differently to the same axon guidance cue when encountering it at a different point in time and space (Kolodkin & Tessier-Lavigne 2011). As an axon grows into new brain regions, it must therefore respond to new cues and often differently to the same previously encountered cue. The molecular mechanisms underlying this variable response to the same cue is poorly understood. We propose that nestin acts as a sensitizer and might provide a gain control mechanism, such that axons lacking nestin are less repelled by Sema3a than axons expressing nestin. At the early developmental time points when nestin expression is observed, we hypothesize that nestin may be important for initial axon positioning in the IZ downstream of Sema3a, which is localized on either side of the IZ in the cortical plate and ventricular zone (Ruediger et al. 2013). Several other molecules have been shown to modulate responsiveness to guidance cues (Kaplan et al. 2014), including types of co-receptors (Dang et al. 2013), lipid raft components (Carcea et al. 2010), second messengers (such as cAMP and calcium), (Henley et al. 2004; Tojima et al. 2014) and modification of downstream signaling cascades by ERM (Mintz et al. 2009), α2-Chimaerin (Brown et al. 2004; Ip et al. 2011), and 14-3-3 proteins(Yam et al. 2012; Kent et al. 2010). Our results now add the IF protein nestin to this category of proteins that can variably regulate responsiveness to Sema3a. The previously identified modulators often serve to vary the degree of signaling output to alter the cytoskeleton and adhesive properties of the growth cone (Vitriol & Zheng 2012). How exactly nestin affects downstream signaling by cdk5 and if there are substrates of cdk5 which might be differentially active in the absence or presence of nestin is currently unknown and will be of great interest to investigate in the future.

Acknowledgements

We thank Brenna Kirk and Pranaya Pakala (Litwa Lab) for work with human IPSCs, Meheret Kinfe for blinded neuron counting, Deppman lab for TUJ1 antibody, Laura Digilio, Lloyd McMahon, Kelly Barford (Winckler Lab), and Austin Keeler (Deppman Lab) for help with manuscript revision and expertise, Zdenek Svindrych of the University of Virginia Keck Center for assistance with STED microscopy, and Bruce Lahn's lab of the University of Chicago for generously providing mouse nestin cDNA. This work was supported by NIH grant R01NS081674 (to BW).

The authors declare no competing financial interests.

CB and BW conceived and coordinated the study, interpreted the data, and wrote the paper. CJ and KA devised, performed and analyzed Human IPSC studies (figure 2B

and S2A). CB devised, performed, and analyzed all other experiments. CY and ND provided critical expertise for experimental design and execution.

Material and methods

Antibodies

Mouse anti-Nestin Rat401- recognizes the unique C-terminal tail region of nestin(Su et al. 2013)–All experiments shown with 2q178 were also repeated with this antibody. Note this antibody and the other antibodies recognize full length nestin. 1:200 IF, 1:500 IHC, 1:500 WB **DSHB Cat# Rat-401 also rat-401 RRID:AB_2235915**

Mouse anti-Nestin 2Q178 This clone and RAT401 produce indistinguishable staining patterns. All staining and blotting is done with this antibody unless otherwise noted. 1:200 IF, 1:500 IHC, 1:500 WB **Santa Cruz Biotechnology Cat# sc-58813 RRID:AB_784786**

Goat anti-Nestin R-20: Raised against peptide in the unique C-terminal tail region of nestin 1:200 IHC **Santa Cruz Biotechnology Cat# sc-21249 RRID:AB_2267112**

Chicken anti-Nestin- three peptide directed antibodies combined to the unique C-terminal tail region of nestin 1:300 IF, 1:400 IHC, 1:3000 WB **Aves Labs Cat# NES RRID:AB_2314882**

Rabbit anti-DCX- 1:1200 IF, IHC, 1:4000 WB **Abcam Cat# ab18723 RRID:AB_732011**

Mouse anti- β3 Tubulin Tuj1- 1:800 IF A generous gift from the Deppman Lab YVA **A. Frankfurter, University of Virginia; Department of Biology Cat# TuJ1 (beta III tubulin) RRID:AB_2315517**

Chicken anti-β3 tubulin- 1:200 IF **Aves Labs Cat# TUJ RRID:AB_2313564**

Rat anti α-tubulin- 1:2000 WB Santa **Cruz Biotechnology Cat# sc-53030 RRID:AB_2272440**

Rabbit anti-Vimentin- 1:100 IF, 1:100 IHC, 1:1000 WB **Bioss Inc Cat# bs-0756R RRID:AB_10855343**

Rat anti-Myc tag 9E1- 1:1000 WB ChromoTek Cat# 9e1-100, RRID:AB_2631398

Mouse anti-NeurofilamentM 2H3- 1:200 IF **DSHB Cat# 2H3 RRID:AB_531793**

Mouse anti-αInternexin 2E3- 1:100 IHC **Sigma-Aldrich Cat# I0282 RRID:AB_477086**

Rat anti-L1- 1:150 IHC **Millipore Cat# MAB5272 RRID:AB_2133200**

Mouse anti-Tag1-4D7 (DSHB) 1:150 IHC **DSHB Cat# 4D7 RRID:AB_2315433**

Rabbit anti-Calretinin- 1:600 IHC **Millipore (chemicon) Cat# PC254L-100UL RRID:AB_564321**

Rat anti-CTIP2- 1:400 IF **BioLegend Cat# 650601 RRID:AB_10896795**

Rabbit anti-SatB2- 1:400 IF **Abcam Cat# ab92446 RRID:AB_10563678**

GFP booster nanobody- 1:600 IF **ChromoTek Cat# gba488-100 RRID:AB_2631434**

Phalloidin 568 1:150 Invitrogen

Neuronal Culture

Primary cultures of cortical neurons were obtained from embryonic day 16 (E16) mouse cortex of either sex as described as approved in the institutional ACUC protocol #3422. Cells were plated on poly-L-lysine coverslips and incubated with DMEM medium with 10% fetal bovine serum. After 8 hrs, the cells were transferred into serum-free medium supplemented with B27 (Invitrogen) and Glutamine and cultured for a total of indicated time periods *in vitro* (DIV). Cells were plated at ~100K cells per 15mm coverslip, and at 50K in the Low Density experiment, or 125k/coverslip in electroporation experiments. Cortical neurons for culture were harvested at E16 prior to glio-genesis- thus non-neuronal glia are rare in these cultures, but occasional nestin/Sox2 positive, GFAP negative persisting neural stem cells were occasionally found.

2d explants were acquired from E16 cortex, but only partially dissociated before plating as described above.

Cells for Sema3a treatment assay were prepared as described above. At 24 or 36 hours, cell were treated with 1nm mouse sema3a (R&D systems) diluted in growth media for 5 minutes prior to fixation. In some experiments, cells were pre-treated with 10um Roscovitine (Cayman Chemical) for 30 minutes prior to Sema3a treatment. Time course experiments were fixed at the indicated time points after plating.

Immunofluorescence

Cells were fixed in 4% Para-PHEM-Sucrose (PPS) for preservation of the cytoskeleton and cellular morphology with prewarmed fixative to 37° C and fixed at 37° C for 20 min. 60mM PIPES, 25mM HEPES, 10mM EGTA, 2mM MgCl2 (PHEM), .12M sucrose, 4% paraformaldehyde pH 7.4. Thorough permeabilization was required for nestin/intermediate filament visualization in neurons. Coverslips were permeabilized with 0.4% triton-X 200 in 1% BSA PBS for 20 min for nestin and intermediate filament staining, or 0.2% triton-X when no Intermediate filaments were being immunostained, and then blocked for 30 min in 10%BSA, 5% normal donkey serum (NDS) in PBS. Primary antibodies were diluted in 1% BSA in PBS, and secondary antibodies in 1%BSA, 0.5% NDS in PBS. Primary antibody were incubated overnight at 4° C, and secondary antibodies for 90 min at room temperature. Appropriate species specific alexa 350, 488, 568, or 647 labeled secondary antibodies raised in Donkey (Invitrogen)

were used for fluorescent labeling. Phalloidin 568 (Invitrogen) at 1:150 was used to visualize F-actin and Dapi to visualize Nuclei. Coverslips were mounted with ProLong Gold(Invitrogen) and imaged with a Zeiss Z1-Observer with a 40x (for population counting) or 63x (for morphology analysis) objective. Images were captured with the Axiocam 503 camera using Zen software (Zeiss) and processed identically within experiments. No non-linear image adjustments were performed.

Histology

Human IPSC derived Cortical Organoids (minibrains) or embryonic E16 mouse brain were dissected and placed in 4% PFA and 6% sucrose in PBS at 4C overnight. Tissue was then cryo-protected by sinking overnight in 30% sucrose. Tissue was imbedded in OCT, and brains cut by coronal cryosection at 16um sections (Zeiss Confocal imaging) or 10um sections (Abberior super-resolution) .Sections were mounted directly on slide, permeabilized with 3% NDS + 0.2% triton-X 100 in PBS for 1 hour, and blocked with 10% BSA for 30 min. Antibodies were diluted in permeabilization buffer with indicated primary antibodies overnight at 4° C, and secondary antibodies 2 hours at room temperature following thorough washing with PBS. Sections were mounted with prolong gold. For peptide blocking negative control experiments, the goat anti-nestin antibody was diluted at 1:100 with the corresponding epitope immunizing peptide (Santa Cruz) at 1:10 and incubated at room temperature for 3 hours. The goat anti-nestin antibody for the non-blocked condition was diluted and incubated similarly but in the absence of peptide. The antibody was then used as described above. Of note, the anti Tag1 IgM antibody has cross reaction with mouse IgG secondary antibodies, so staining with mouse IgG and mouse IgM antibodies were done sequentially. Confocal imaging of cryosections was carried out on an inverted Zeiss LSM880 confocal microscope using a 63X objective. Super-resolution STED imaging utilized and Abberior STED confocal with 100X objective at the Keck Center and University of Virginia. A donkey ani-goat 488 (Invitrogen) secondary antibody was imaged using a 595 nm extinction laser.

Neuron nucleofection

After cell were dissociated from cortex, but prior to plating, cells were electroporated by Amaxa 4d nucleofection, according to protocol. 800K cell were electroporated in the small volume (20ul) cuvettes using P3 primary cell solution and EM-100, CL-133, and CU-100 programs variably between experiments. All three of these programs worked similarly in our hands. 0.1ug of GFP plasmid (pCMV-GFP-Clonetech) as a transfection marker, and 100nM siRNA (siNes smart-pool Dharmacon siGenome M-057300-01-0010, siCON-SCBT sc-37007).

Cloning

Circular mouse nestin cDNA was obtained as a gift from Bruce Lahn. Briefly, PCR was used to generate ECOR1 and HINDII sites on the 5' or 3" end respectively of full length mouse nestin. Both the insert and vector were treated with EcoR1 and HindII, the cut insert was ligated into pCDNA3.1 Myc-His(+) B.

Cell culture and transfection.

HEK293 cells were maintained in DMEM+10% fetal bovine serum, and all transfections were conducted using Lipofectamine 2000 (Invitrogen) according to the manufacturer's protocol. mNestin-myc and respective control or nestin siRNAs were transfected simultaneously.

Western Blot

Cells were washed with ice cold PBS, and lysed directly on the plate (6cm) into lysis buffer(400ull); 50mM Tris HCl, 150mM NaCl, 1% NP-40, 1mM EDTA, 1mM DTT, 1mM PMSF, 1X HALT protease/phosphatase inhibitor cocktail. After rotisserie at 4° C for 30 minutes, lysate were cleared by centrifugation at 21K X g for 15 min at 4° C. Supernatants were diluted with 5X laemmli buffer and equivalent amounts were run on a 4-20% polyacrylamide gel. After transfer onto nitrocellulose with the BioRad Transblot, membrane was blocked with Licor TBS blocking buffer for 1 hours at room temp. Primaries and secondary antibodies were diluted in 50% blocking buffer, 50% PBS, 0.1% tween-20. Primaries overnight incubation at 4° C, and near-infrared secondary antibodies 1 hour at room temperature. Blot were imaged with the Licor Odyssey CLx imager.

Image analysis

Image J was used for all image analysis

Neuron morphology and nestin expression analysis. Neuron staging was performed according to the Banker neuron staging method, and neurites were called an axon if it is 2X longer than the next longest neurite (dendrite). Nestin positivity in the axon of neurons was assessed by outlining the distal region of the axon and measuring the maximum nestin immuno-staining in the region. This value was used to bin corresponding morphological measurements by nestin intensity. In siRNA experiments, only green GFP+ (transfection indicator) cells were imaged and counted for both for morphology and nestin siRNA efficiency analysis. All counts were confirmed by blinded analysis.

Filopodial protrusion were counted using the phalloidin channel, and any actin rich protrusion from the growth cone was counted. A growth cone was counted as collapsed if it had 0 filopodial protrusions.

Axon length was the length of the axon from the cell body to the growth cone tip

Growth cone area and perimeter were assessed by measuring traced outlines the growth cone not counting the filopodial protrusions, and extending down to where the microtubules consolidate into axon shaft.

Mouse Neural stem cell marker expression. DCX, nestin, and Dapi stained differentiated neural stem cells were manually counted for immunopositivity in any part of the cell above background levels.

Human IPSC Nestin and BIII tubulin co-localization was assessed per image using the ImageJ co-localization plugin.

Mouse neural stem cell culture

Embryonic (E16) cortical neural stem cells were prepared as described(Pacey et al. 2006) and grown as neurospheres for at least 3 passages prior to use for dissociated and differentiating cell experiments to ensure purity. For these experiments, neurospheres were dissociated using Stem Cell chemical dissociated kit, and plated in PLL coated coverslips for 1 day and fixed and immunostained as described. For 4DIV, proliferative media was replaced with media lacking EGF and FGF growth factors until 4 DIV, fixed and processed for immunostaining as described.

Neural Differentiation of Human Induced Pluripotent Stem Cells

Human induced pluripotent stem cells from neurotypic control 9319 were generated by Kristen Brennand in the laboratory of Dr. Fred Gage (Salk Institute). Neural progenitor cells (NPCs) were generated through an embryoid body protocol as described by Brennand et al. PMID: 21490598. For neuronal differentiation, we plated 75,000 control NPCs on each poly-ornithine and laminin-coated 18mm glass coverslip. After 24 hours, cells were switched to neuronal differentiation media consisting of DMEM F12 + Glutamax and supplemented with N2 and B27 with retinoid acid and 20ng/ml BDNF, 20ng/ml GDNF, 400uM cyclic AMP, and 200nM ascorbic acid. Half of the media was replaced with fresh media every 3 days. Neurons were fixed with 4% formaldehyde with 4% sucrose on the days indicated in the text and used for subsequent immunofluorescence analysis.

Generation of Cortical Organoids

Human fibroblasts from neurotypic control 7545 were obtained from the Coriell Institute and reprogrammed into induced pluripotent stem cells by the laboratory of Dr. Mike McConnell (UVa) using the CytoTune Reprogramming Kit (Life Technologies) and maintained in Essential 8 media (Life Technologies). Cortical organoids were grown using a low-attachment protocol[20]. Briefly, we used dispase to detach hIPSC colonies from matrigel dishes. These colonies were placed in ES/DMEM

media (GlobalStem) supplemented with 20% Knockout Serum Replacement (Life Technologies) and treated with 5mM Dorsomorphin and 10mM SB-431542 for the first 5 days. The ROCK inhibitor, 10mm Y-27632, was added for the first 48 hours. From day 6-24, spheroids were fed with Neuronal Media consisting of Neurobasal A with B27 without Vitamin A, GlutaMax, penicillin/streptomycin (Life Technologies), and supplemented with 20ng/ml EGF and FGF2 (Peprotech). From day 25-42, the growth factors were replaced with 20ng/ml BDNF and NT3 (Peprotech). From Day 43 onwards, BDNF and NT3 were removed and organoids were grown solely in Neuronal Media.

Statistical analysis

Human IPSC Nestin and Beta3 tubulin colocalization was performed using Sigma Plot 13.0. All other statistical analysis was carried out using Prism software. Datasets were first evaluated as parametric versus nonparametric. As indicated in the figure legends, the corresponding one way ANOVA test was used when there were multiple comparisons, and the t-test was used when only two conditions were compared.

References

Banker, G.A. & Cowan, W.M., 1977. Rat Hippocampal neurons in dispersed cell culture. *Brain Research*, 126(3), pp.397–425.

Boyne, L.J., Fischer, I. & Shea, T.B., 1996. Role of vimentin in early stages of neuritogenesis in cultured hippocampal neurons. *International Journal of Developmental Neuroscience*, 14, pp.739–748.

Brown, M. et al., 2004. α2-Chimaerin, Cyclin-Dependent Kinase 5/p35, and Its Target Collapsin Response Mediator Protein-2 Are Essential Components in Semaphorin 3A-Induced Growth-Cone Collapse. *The Journal of Neuroscience*, 24(41), pp.8994–9004.

Carcea, I. et al., 2010. Flotillin-Mediated Endocytic Events Dictate Cell Type-Specific Responses to Semaphorin 3A. *Journal of Neuroscience*, 30(45), pp.15317–15329. Available at: http://www.jneurosci.org/cgi/doi/10.1523/JNEUROSCI.1821-10.2010.

Crews, L. et al., 2011. Modulation of aberrant CDK5 signaling rescues impaired neurogenesis in models of Alzheimer's disease. *Cell death & disease*, 2(2), p.e120. Available at: http://www.pubmedcentral.nih.gov/articlerender.fcgi?artid=3101702&tool=pmcentrez&rendertype=abstract [Accessed December 17, 2014].

Dang, P., Smythe, E. & Furley, A.J.W., 2013. TAG1 regulates the endocytic trafficking and signalling of the Semaphorin3A receptor complex. *Journal of Neuroscience*, 32(30), pp.10370–10382.

Dent, E.W., 2004. Netrin-1 and Semaphorin 3A Promote or Inhibit Cortical Axon Branching, Respectively, by Reorganization of the Cytoskeleton. *Journal of Neuroscience*, 24(12), pp.3002–3012. Available at: http://www.jneurosci.org/cgi/doi/10.1523/JNEUROSCI.4963-03.2004.

Digilio, L. Yap, CC. Winckler, B., 2015. Ctip2-, Satb2-, Prox1-, and GAD65-Expressing Neurons in Rat Cultures: Preponderance of Single- and Double-Positive Cells, and Cell Type-Specific Expression of Neuron-Specific Gene Family Members, Nsg-1 (NEEP21) and Nsg-2 (P19). *PloS one*, pp.1–16.

Dotti, C.G., Sullivan, C. a & Banker, G. a, 1988. The establishment of polarity by hippocampal neurons in culture. *The Journal of neuroscience : the official journal of the Society for Neuroscience*, 8(4), pp.1454–1468.

Francis, F. et al., 1999. Doublecortin is a developmentally regulated, microtubule-associated protein expressed in migrating and differentiating neurons. *Neuron*, 23(2), pp.247–256.

Hemmati-Brivanlou, A., Mann, R.W. & Harland, R.M., 1992. A protein expressed in the growth cones of embryonic nerves defines a new class of intermediate filament

protein. *Neuron*, 9(3), pp.417–428.

Hendrickson, M.L. et al., 2011. Expression of nestin by neural cells in the adult rat and human brain. *PloS one*, 6(4), p.e18535. Available at: http://www.pubmedcentral.nih.gov/articlerender.fcgi?artid=3072400&tool=pmcentrez&rendertype=abstract [Accessed December 17, 2014].

Henley, J.R. et al., 2004. Calcium mediates bidirectional growth cone turning induced by myelin-associated glycoprotein. *Neuron*, 44(6), pp.909–916.

Hockfield, S. & McKay, R.D., 1985. Identification of major cell classes in the developing mammalian nervous system. *The Journal of neuroscience : the official journal of the Society for Neuroscience*, 5, pp.3310–3328.

Holmgren, A. et al., 2013. Charcot-Marie-Tooth causing HSPB1 mutations increase Cdk5-mediated phosphorylation of neurofilaments. *Acta Neuropathologica*, 126(1), pp.93–108.

Ip, J.P.K. et al., 2011. a 2-chimaerin controls neuronal migration and functioning of the cerebral cortex through CRMP-2. *Nature Neuroscience*, 15(1), pp.39–47. Available at: http://dx.doi.org/10.1038/nn.2972.

Kaplan, A. et al., 2014. Switching Responses : Spatial and Temporal Regulators of Axon Guidance. *Molecular Neurobiology*, pp.1077–1086.

Kaplan, P. et al., 1990. α-Internexin, a Novel Neuronal Intermediate Filament Protein , Precedes the Low Molecular Weight Neurofilament Protein (NF-L) in the Developing Rat Brain. *The Journal of Neuroscience*, (August).

Kawauchi, T., 2014. Cdk5 regulates multiple cellular events in neural development, function and disease. *Development, growth & differentiation*, 56(5), pp.335–48. Available at: http://www.ncbi.nlm.nih.gov/pubmed/24844647 [Accessed December 17, 2014].

Kent, C.B. et al., 2010. 14-3-3 Proteins Regulate Protein Kinase A Activity to Modulate Growth Cone Turning Responses. *The Journal of Neuroscience*, 30(42), pp.14059–14067.

Kobayashi, H. et al., 2014. Phosphorylation of Cyclin-dependent Kinase 5 (Cdk5) at Tyr-15 Is Inhibited by Cdk5 Activators and Does Not Contribute to the Activation of Cdk5 *. *The Journal of biological chemistry*, 289(28), pp.19627–19636.

Kolodkin, A.L. & Tessier-Lavigne, M., 2011. Mechanisms and molecules of neuronal wiring: a primer. *Cold Spring Harbor perspectives in biology*, 3(6). Available at: http://www.pubmedcentral.nih.gov/articlerender.fcgi?artid=3098670&tool=pmcentrez&rendertype=abstract [Accessed August 29, 2014].

Lariviere, R.C. & Julien, J., 2003. Functions of Intermediate Filaments in Neuronal Development and Disease. *Journal of Neurobiology*.

Leduc, C. & Manneville, S.E., 2017. Regulation of microtubule-associated motors drives intermediate filament network polarization. *The Journal of Cell Biology*.

Lee, S. & Shea, T.B., 2014. The high molecular weight neurofilament subunit plays an essential role in axonal outgrowth and stabilization. *Biology open*, 3(10), pp.974–81. Available at: http://www.pubmedcentral.nih.gov/articlerender.fcgi?artid=4197446&tool=pmcentrez&rendertype=abstract.

Lendahl, U., Zimmerman, L.B. & McKay, R.D.G., 1990. CNS stem cells express a new class of intermediate filament protein. *Cell*, 60(4), pp.585–595. Available at: http://www.sciencedirect.com/science/article/pii/009286749090662X.

Lin, W. et al., 2005. Neurotransmitter Acetylcholine Negatively Regulates Neuromuscular Synapse Formation by a Cdk5-Dependent Mechanism. *Neuron*, 46, pp.569–579.

Mintz, C.D. et al., 2009. ERM proteins regulate growth cone responses to Sema3A. *J Comp Neurol*, 510(4), pp.351–366.

Mohseni, P. et al., 2011. Nestin is not essential for development of the CNS but required for dispersion of acetylcholine receptor clusters at the area of neuromuscular junctions. *The Journal of neuroscience : the official journal of the Society for Neuroscience*, 31(32), pp.11547–52. Available at: http://www.ncbi.nlm.nih.gov/pubmed/21832185 [Accessed December 17, 2014].

Namba, T. et al., 2014. Pioneering axons regulate neuronal polarization in the developing cerebral cortex. *Neuron*, 81(4), pp.814–829. Available at: http://dx.doi.org/10.1016/j.neuron.2013.12.015.

Ng, T. et al., 2013. Class 3 Semaphorin Mediates Dendrite Growth in Adult Newborn Neurons through Cdk5/FAK Pathway. *PLoS ONE*, 8(6), pp.1–15.

Pacey, L. et al., 2006. Neural Stem Cell Culture: Neurosphere generation, microscopical analysis and cryopreservation. *Nature Protocol Exchange*. Available at: http://dx.doi.org/10.1038/nprot.2006.215.

Pallari, H. et al., 2011. Nestin as a regulator of Cdk5 in differentiating myoblasts. *Molecular biology of the cell*, 22.

Perry, E.K. et al., 2012. Neurogenic abnormalities in Alzheimer's disease differ between stages of neurogenesis and are partly related to cholinergic pathology. *Neurobiology of Disease*, 47(2), pp.155–162.

Romito-DiGiacomo, R.R. et al., 2007. Effects of Alzheimer's disease on different cortical layers: the role of intrinsic differences in Abeta susceptibility. *The Journal of neuroscience : the official journal of the Society for Neuroscience*, 27(32), pp.8496–504. Available at: http://www.ncbi.nlm.nih.gov/pubmed/17687027 [Accessed December 17, 2014].

Ruediger, T. et al., 2013. Integration of opposing semaphorin guidance cues in cortical axons. *Cerebral Cortex*, 23(3), pp.604–614.

Sahlgren, C.M. et al., 2006. A nestin scaffold links Cdk5/p35 signaling to oxidant-induced cell death. *The EMBO journal*, 25(20), pp.4808–19. Available at:

http://www.pubmedcentral.nih.gov/articlerender.fcgi?artid=1618100&tool=pmcentrez&rendertype=abstract [Accessed December 17, 2014].

Sahlgren, C.M. et al., 2003. Cdk5 Regulates the Organization of Nestin and Its Association with p35. *Molecular and cellular biology*, 23(14), pp.5090–5106.

Sasaki, Y. et al., 2002. Fyn and Cdk5 mediate semaphorin-3A signaling, which is involved in regulation of dendrite orientation in cerebral cortex. *Neuron*, 35(5), pp.907–920.

Shea, T.B. & Beermann, M.L., 1999. Neuronal intermediate filament protein alpha-internexin facilitates axonal neurite elongation in neuroblastoma cells. *Cell motility and the cytoskeleton*, 43(4), pp.322–333. Available at: (null).

Shea, T.B., Beermann, M.L. & Fischer, I., 1993. Transient Requirement for Vimentin in Neuritogenesis : Intracellular Delivery of Anti-Vimentin Antibodies and Antisense Oligonucleotides Inhibit Neurite Initiation But Not Elongation of Existing Neurites in Neuroblastoma. *Journal of neuroscience research*, 76, pp.66–76.

Sibbe, M. et al., 2007. Development of the corticospinal tract in Semaphorin3A- and cd24-deficient mice. *Neuroscience*, 150, pp.898–904.

Steinert, P.M. et al., 1999. A High Molecular Weight Intermediate Filament-associated Protein in BHK-21 Cells Is Nestin, a Type VI Intermediate Filament Protein: Limited Co-assembly in vitro to form Heteropolymers with TypeII Vimentin and Type IV alpha-Internexin. *Journal of Biological Chemistry*, 274(14), pp.9881–9890. Available at: http://www.jbc.org/content/274/14/9881.abstract.

Su, P.-H. et al., 2013. Identification and cytoprotective function of a novel nestin isoform, Nes-S, in dorsal root ganglia neurons. *The Journal of biological chemistry*, 288(12), pp.8391–404. Available at: http://www.pubmedcentral.nih.gov/articlerender.fcgi?artid=3605656&tool=pmcentrez&rendertype=abstract [Accessed December 17, 2014].

Takebayashi, H. et al., 2015. Draxin from neocortical neurons controls the guidance of thalamocortical projections into the neocortex. *Nature Communications*, 6, pp.1–13. Available at: http://dx.doi.org/10.1038/ncomms10232.

Tojima, T., Itofusa, R. & Kamiguchi, H., 2014. Steering neuronal growth cones by shifting the imbalance between exocytosis and endocytosis. *The Journal of neuroscience : the official journal of the Society for Neuroscience*, 34(21), pp.7165–78. Available at: http://www.ncbi.nlm.nih.gov/pubmed/24849351 [Accessed December 2, 2014].

Toth, C. et al., 2008. Ndel1 promotes axon regeneration via intermediate filaments. *PLoS ONE*, 3(4).

Uchida, A., Alami, N.H. & Brown, A., 2009. Tight Functional Coupling of Kinesin-1A and Dynein Motors in the Bidirectional Transport of Neurofilaments. *Molecular biology of the cell*, 20, pp.4997–5006.

Vitriol, E. a. & Zheng, J.Q., 2012. Growth Cone Travel in Space and Time: The Cellular

Ensemble of Cytoskeleton, Adhesion, and Membrane. *Neuron*, 73(6), pp.1068–1080. Available at: http://www.pubmedcentral.nih.gov/articlerender.fcgi?artid=3319373&tool=pmcentrez&rendertype=abstract [Accessed December 2, 2014].

Walker, K.L. et al., 2001. Loss of neurofilaments alters axonal growth dynamics. *The Journal of neuroscience : the official journal of the Society for Neuroscience*, 21(24), pp.9655–66. Available at: http://www.ncbi.nlm.nih.gov/pubmed/11739575.

Walker, T.L. et al., 2007. The Doublecortin-Expressing Population in the Developing and Adult Brain Contains Multipotential Precursors in Addition to Neuronal-Lineage Cells. *The Journal of Neuroscience*, 27(14), pp.3734–3742.

Wang, L. et al., 2000. Rapid movement of axonal neurofilaments interrupted by prolonged pauses. *Nature Cell Biology*, 2(March), pp.137–141.

Xia, C. et al., 1988. Abnormal neurofilament transport caused by targeted disruption of neuronal kinesin heavy chain KIF5A. *The Journal of Cell Biology*, pp.55–66.

Yabe, J.T. et al., 2003. Regulation of the Transition From Vimentin to Neurofilaments During Neuronal Differentiation. *Cell Motility and the Cytoskeleton*, 56(March), pp.193–205.

Yabe, J.T. et al., 2001. Selective accumulation of the high molecular weight neurofilament subunit within the distal region of growing axonal neurites. *Cell Motility and the Cytoskeleton*, 50(February), pp.1–12.

Yam, P.T. et al., 2012. 14-3-3 Proteins Regulate a Cell-Intrinsic Switch from Sonic Hedgehog-Mediated Commissural Axon Attraction to Repulsion after Midline Crossing. *Neuron*, pp.735–749.

Yan, Y. et al., 2001. Mouse nestin protein localizes in growth cones of P19 neurons and cerebellar granule cells. *Neuroscience letters*, 302(2–3), pp.89–92. Available at: http://www.ncbi.nlm.nih.gov/pubmed/11290394.

Yang, J. et al., 2011. Nestin negatively regulates postsynaptic differentiation of the neuromuscular synapse. *Nature neuroscience*, 14, pp.324–30. Available at: http://www.pubmedcentral.nih.gov/articlerender.fcgi?artid=3069133&tool=pmcentrez&rendertype=abstract.

Figure Legends:

Figure 1: *Nestin protein expression persists in immature primary cortical neurons in culture.*

A. Nestin expression in cultures derived from E16 mouse cortex grown for one day (1DIV). Doublecortin (DCX) immunostaining and a stage 3 morphology was used to identify neurons. Nestin is enriched near the axonal growth cone (pink arrowheads), but largely absent from growth cones of minor dendrites (white arrows) using both mouse and chicken anti-nestin antibodies. White arrowheads indicate short nestin IF segments found along the axon shaft.

B. Validation of nestin antibody staining on stage3 neurons with mouse and goat anti-nestin antibodies with immunizing peptide antibody blocking. Both antibodies again show a distal axon enrichment of nestin (pink arrowheads) while the dendrites again are not labeled (white arrows). Pre-incubation of the goat anti-nestin antibody with the immunizing peptide abolishes all staining but staining in the distal axons is still detectable with the mouse anti-nestin antibody which was raised against a different epitope. Shown are E16 mouse cortical neurons 1DIV. White arrowheads indicate short nestin IF segments in axon shaft.

C. Nestin siRNA results in loss of immunostaining, validating that the axonal growth cone staining is due to nestin protein. GFP was co-transfected as a transfection indicator, and nestin immunostaining was quantified in stage 3 neurons. ~1/3 of siCon neurons express nestin at 36 hrs in the distal axon (pink arrowheads). Very few transfected neurons showed nestin enrichment in the axon under nestin siRNA conditions (white arrowheads). 120-140 cells per condition were counted in n=5 independent experiments. $p < 0.001$ (Paired t-test).

D. Nestin is co-localized with other intermediate filaments in the same assembly group (vimentin and Neurofilament-Medium NEFM) in the distal axon (pink arrowheads) of E16 mouse cortical neurons 1DIV. High magnification of the boxed region and linescans reveal that nestin and NEFM appear to decorate the same filament structure in partially co-localizing subdomains, as expected for nestin containing intermediate filaments. Pink arrowheads indicate nestin positive axonal intermediate filament heteropolymers.

Figure 2: *Nestin-expressing neurons are observed in multiple rodent and human culture models*

A. Mouse Neurosphere NPC cultures: Nestin expression was assessed in differentiating dissociated neural progenitor cells (mouse NPC) after 4 days of neuronal differentiation. DCX-positive neurons frequently stain positive for nestin (yellow asterisk), especially in axon tips (pink arrowheads). A axon single positive for DCX but not nestin is marked with a series of white arrowheads along the length of the long and thin axon. Nestin single positive cells are marked with a pink asterisk. One example of a double-positive cell is shown in the middle panels to highlight its neuronal morphology and tip-enriched nestin staining (pink arrowhead). The proportion of cells positive for only nestin (red bar), only DCX (green bar) or double-positive for DCX and nestin (yellow bar) was quantified for NPCs cultured under differentiation conditions from 1 or 4 days. Yellow dotted lines highlight the expanding double positive population (yellow bar). 323 cells were counted at 1 DIV, and 219 cells counted at 4 DIV.

B. Human IPSC derived neuronal cultures: Nestin is expressed in human (IPSC) differentiating neurons derived from NPCs in dissociated cultures under differentiating conditions from 1, 4 and 6 days. The distribution of nestin is similar to the mouse NPC-derived neurons described above. Percent co-localization with the neuronal-specific β3 tubulin was quantified. A close-up of a nestin-positive axon tip in the boxed region is shown in the panels below the respective image. n=14 (day 1), 10 (day 4), and 14 (day 6-8). (Mann-Whitney)

C. Mouse primary neurons cortical neuron cultures: Percentage of nestin-positive neurons decreases with time in culture, but does not vary by density (LD= Low density) at 24hrs. (120 stage 3 neurons were counted per time point for 2 experiments). Cortical neuron cultures were prepared from E16 mice embryos and culture times are indicated.

D. Mouse primary explants: Axonal nestin expression is progressively lost between 36 to 72hours in culture. Significant axonal nestin immunostaining is no longer detected by 72 hours. E16 mouse cortex was explanted by incomplete dissociation and cultured. Axon fascicles emerging from the explant are shown. Arrowheads point at axon tips.

Figure 3: Nestin is expressed in sub-populations of cortical axons in developing cortex.

A. A low magnification of a coronal cortical section (E16 mouse) is shown for orientation (top) and showing α-internexin localization to the axon rich intermediate zone. The white box (lateral lower Intermediate Zone) is the region imaged in the following panels, and is diagramed below illustrating the vertically oriented radial glia, and horizontal IZ axon bundles.

B. Nestin staining of the lower intermediate zone of E16 mouse cortex using chicken anti-nestin (aqua) and goat anti-nestin (pink) antibodies. Axon tracts are visualized

with α-internexin antibody (white). Nestin staining is found in radial glia fibers (arrowheads) as well as in α-internexin-positive axon tracts (arrows). The goat anti-nestin antibody was preincubated with immunizing peptide on sequential cryosections in the lower panels. All staining with the goat anti-nestin antibody was blocked by peptide preincubation, including the axon tract staining, demonstrating that the axon staining was specific and not background staining. All images correspond to higher magnification of the lower intermediate zone of the lateral E16 mouse cortex (boxed regions in A). Radial glia are oriented vertically (arrowheads) and axon tracts are oriented horizontally (arrows).

C. Nestin (multiple antibodies) is found together with its polymerization partner vimentin along axons (identified by the axonal cell adhesion molecule L1-CAM). Arrow heads indicate radial glia and arrows indicate nestin-positive axons.

D. Super resolution microscopy (STED) of nestin immunostaining reveals bright staining of radial glial fibers (arrowheads) as well as fainter staining of axons (arrows) in mouse E16 cortex. Many axons in the axon fascicle do not express nestin, so only a subset of axons in the intermediate zone express nestin at this time point. Arrow heads indicate radial glia and arrows indicate nestin-positive axons.

E. Identification of nestin-positive axons in mouse cortex. The L1-CAM-positive axons (white) contain mixed populations of both cortical and thalamic projections in this brain region. Nestin (magenta) is specifically expressed in axons originating from the cortex (tag-1-positive; blue), but not in axons with thalamic origin (calretinin-positive, yellow). Arrow heads indicate radial glia and arrows indicate nestin-positive and Tag1-positive axons.

Figure 4: Nestin-expressing neurons have smaller growth cones with fewer filopodia, and are more sensitive to Sema3a in a cdk5 dependent manner.

A. E16 mouse cortical neurons 1DIV (stage 3) were immunostained against DCX (to confirm neuronal identity), phalloidin (to visualize the growth cones), and nestin. Cells were binned into thirds by distal axon nestin intensity Nes(-)-not detected, Nes(+)-low expression, and Nes(++)-high expression. Insets allow for appreciation of the filamentous nature of the nestin immunostaining. Channel intensity is adjusted equally for nestin and DCX. In the low magnification, phalloidin labeling has been adjusted variably to show morphology, but in the insets the phalloidin channel was adjusted in an equal manner. Neuron morphology was quantified (40 cells per bin total over 4 independent experiments). Nestin expressing neurons are not significantly different by axon length (B), but have significantly smaller axon growth cones (C). Mean and SD are indicted. Statistical test was Kruskal-Wallis test with n=4.

D. E16 mouse cortical neurons 1DIV (stage 3) were treated for 5 minutes with 1 nM Sema3a and then fixed and immunostained against DCX (to confirm neuronal identity), phalloidin (to visualize the growth cones), and nestin. Cells were binned into thirds by nestin intensity Nes(-)-not detected, Nes(+)-low expression, and Nes(++)-high expression. Insets demonstrate the fragmented appearance of nestin after Sema3a treatment. Growth cone collapse and filopodia number were quantified for 4 experiments. The average of 30 cells quantified per experiment is shown. Roscovitine to inhibit cdk5 was included in two experiments. Growth cones collapse significantly (Kruskal-Wallis test) after 5min 1nM Sema3a treatment, but not when pretreated with 10uM Roscovitine for 30min prior to Sema3a treatment (E). Of the 1/4 of growth cones that collapsed after Sema3a treatment, all have nestin. Neurons with more nestin have higher rates of collapse after Sema3a treatment, and significantly so in the high nestin expressing bin (F). (Friedman test) Nestin expressing neurons have significantly fewer filopodia, and have significantly fewer filopodia after Sema3a treatment, whereas nestin negative neurons do not respond to Sema3a treatment (G). (one way ANOVA).

Figure5: Nestin siRNA results in abnormal growth cone morphology and resistance to Sema3a.

A. Primary E16 Mouse cortical neurons were co-transfected with a plasmid encoding GFP and either control siRNA or nestin siRNA and cultured for 36hrs. GFP booster was used to visualize transfected cells, Tuj1 (β3-tubulin) was used to confirm neuronal identity and for cell morphology, and phalloidin to visualize growth cones. The efficiency of nestin knockdown was quantified in Figure 1C. Nestin siRNA treated cells had no significant difference in axon length (B) but had significantly larger growth cones (C). 100 – 120 cells (plotted on the graph) were measured and averaged for each experiment and each condition. 4 independent experiments were averaged and n=4 was used for statistical analysis (Paired t-test)

D. E16 mouse cortical neurons 1DIV (stage 3) were co-transfected with a plasmid encoding GFP and either control siRNA or nestin siRNA and cultured for 36hrs and then treated for 5 minutes with 1 nM Sema3a. Approximately 40% of control growth cones collapse at 36 hours in culture after Sema3a treatment (significant compared to untreated siCON or Sema3a treated siNes-(Kruskal-Wallis test) , whereas nestin siRNA treated cells had negligible numbers of collapsed growth cones (E). Nestin siRNA resulted in more filopodia per growth cone, and these filopodia were resistant to Sema3a retraction (F) (One way ANOVA). Quantification was carried out for 100 – 120 cells per condition. 4 independent experiments were averaged and n=4 was used for statistical analysis.

Figure 1: Nestin protein expression persists in immature primary cortical neurons in culture.

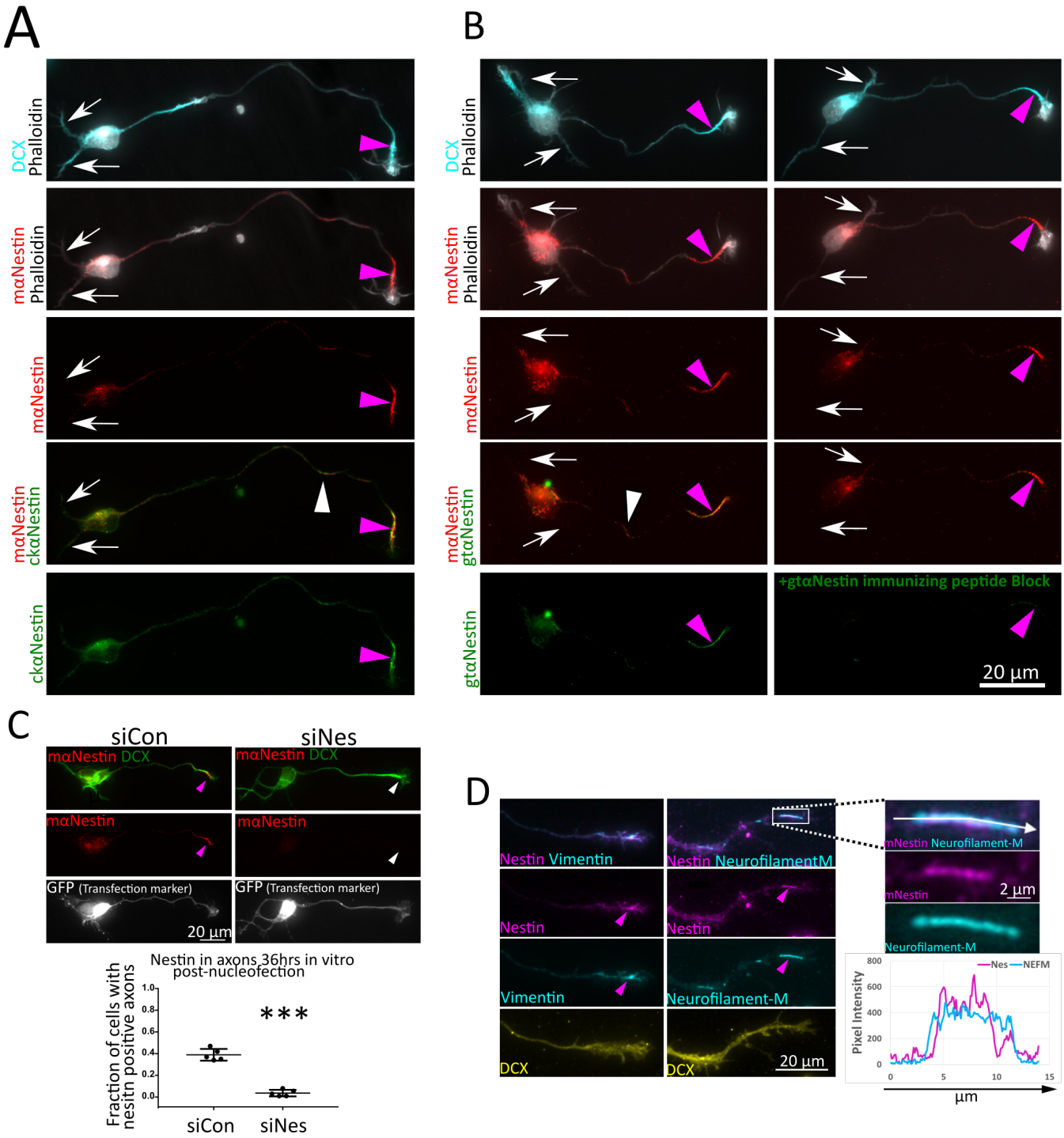

Figure2: Nestin-expressing neurons are observed in multiple rodent and human culture models

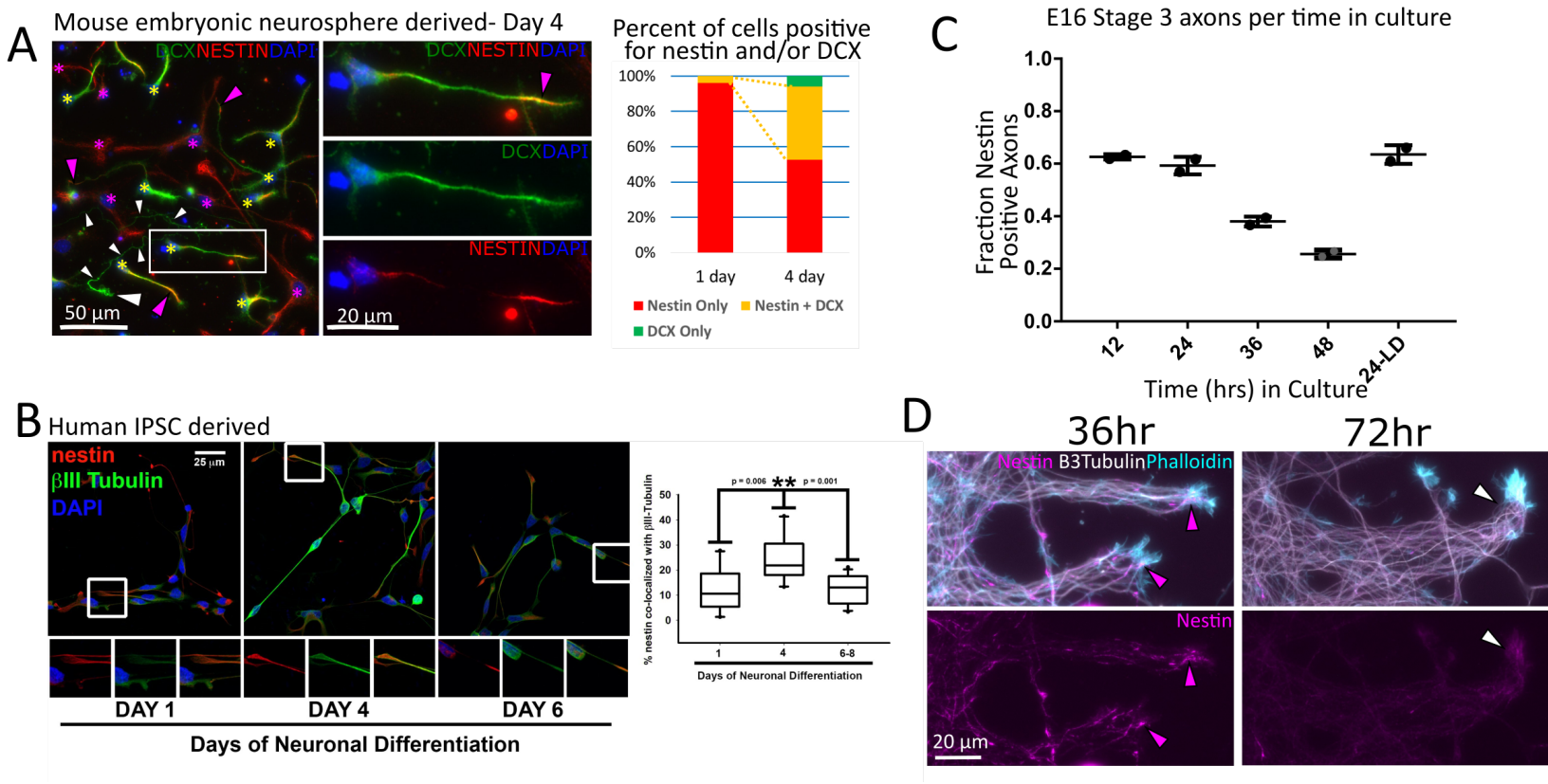

Figure 3:Nestin is expressed in sub-populationsof cortical axons in developing cortex.

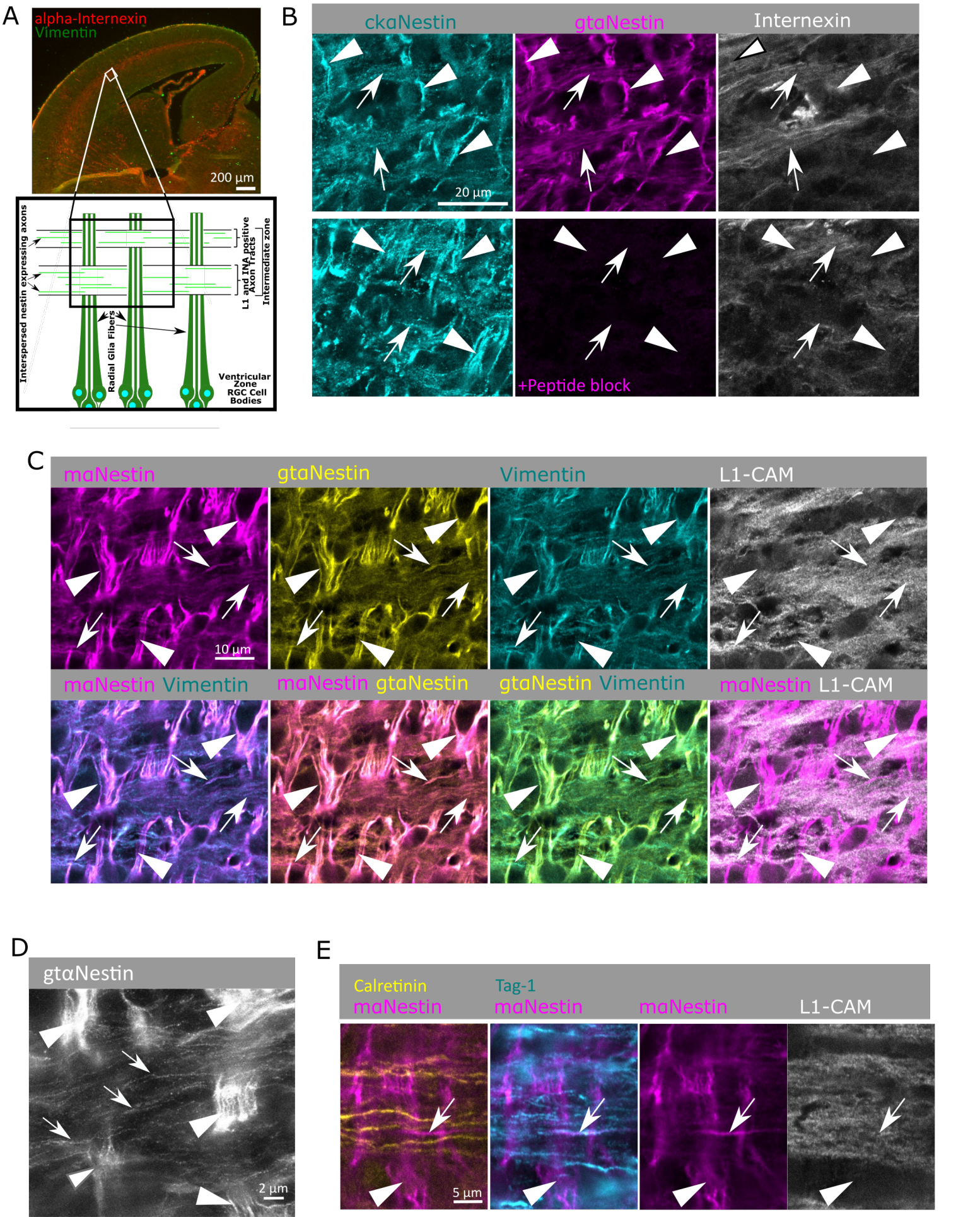

Figure 4: The level of nestin expression in neurons influences growth cone morphology and response to Semaphorin3a.

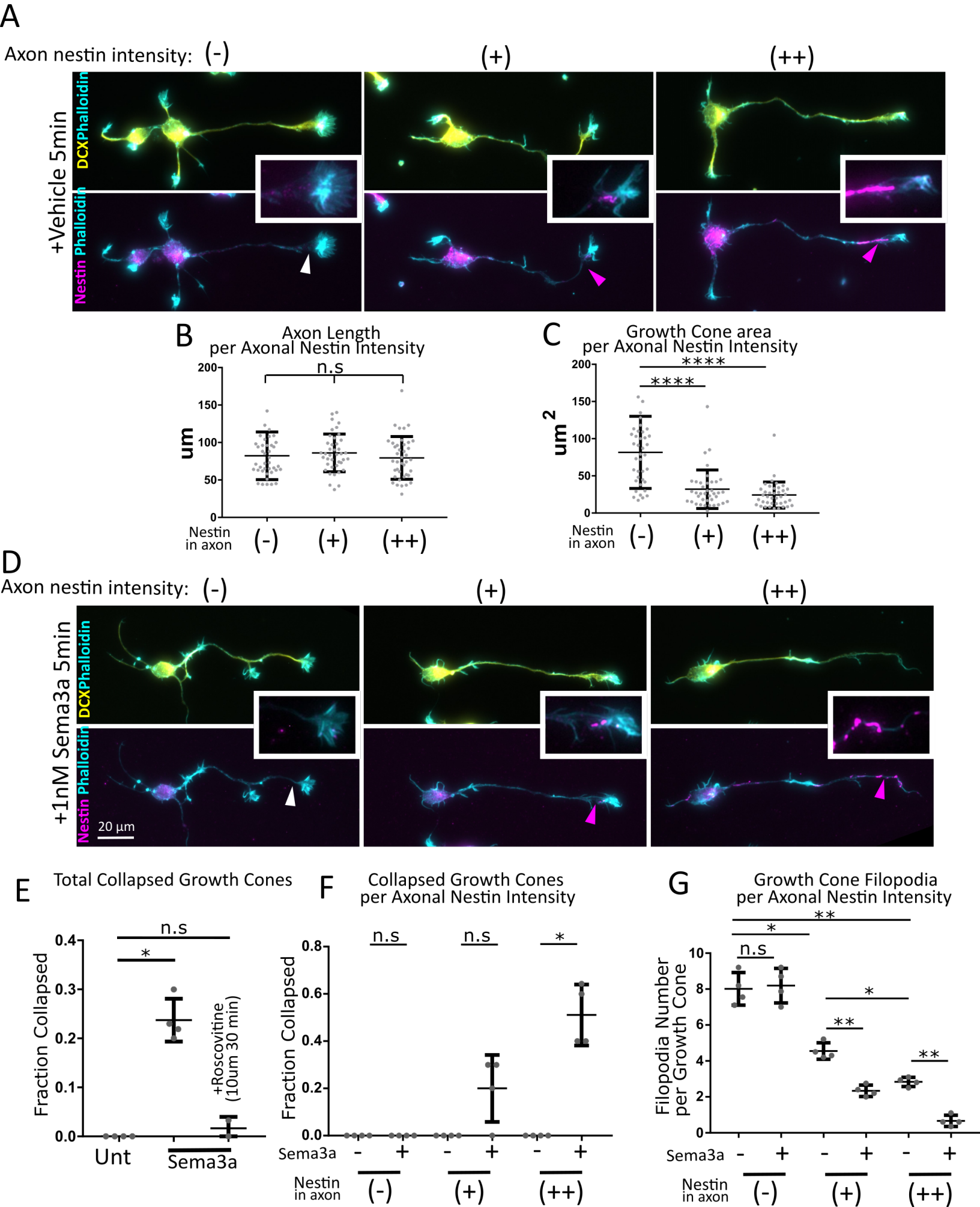
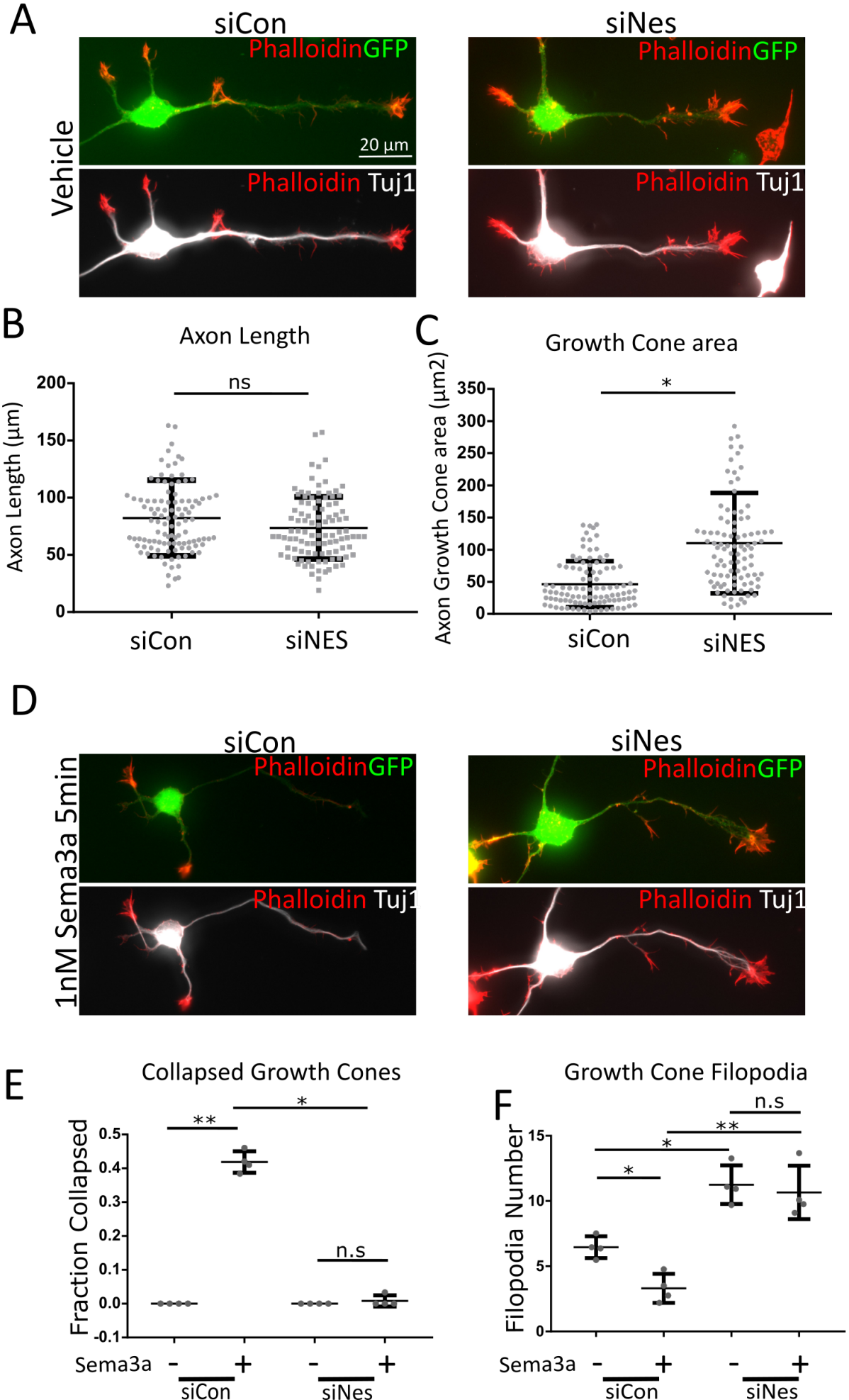
Figure5: Nestin depletion results in abnormal growth cone morphology and resistance to Semaphorin3a.